Sheared edge formability characterization of cold-rolled advanced high strength steels for automotive applications

To cite this article: A Lara *et al* 2022 *IOP Conf. Ser.: Mater. Sci. Eng.* **1238** 012029

Sheared edge formability characterization of cold-rolled advanced high strength steels for automotive applications

A Lara[1], D Frómeta[1], S Parareda[1], D Casellas[1,2], P Larour[3], J Hinterdorfer[3], E Atzema[4] and M Heuse[5]

[1] Eurecat, Centre Tecnològic de Catalunya, Plaça de la Ciència, 2, Manresa 08243, Spain
[2] Luleå University of Technology, 971 87 Luleå, Sweden
[3] voestalpine Stahl GmbH, voestalpine-Straße 3, 4020 Linz, Austria
[4] Tata Steel, P.O. Box 10.000, 1970 CA IJmuiden, The Netherlands
[5] Faurecia Autositze GmbH, Garbsener Landstraße 7, 30419 Hannover, Germany

E-mail: toni.lara@eurecat.org

Abstract. Edge cracking has become a limiting factor in the use of some advanced high strength steels (AHSS) for high-performance automotive applications. This fact has motivated the development of a multitude of experimental tests for edge formability prediction over the last years. In this sense, the Hole Expansion Test (HET) according to ISO16630 has been established in the automotive industry as a standard procedure for edge cracking sensitivity ranking. However, whereas it may be useful for rapid material screening, the results are often not accurate and reliable enough. Consequently, alternative methods based on Digital Image Correlation (DIC) have been proposed aimed at improving the prediction of edge cracking occurrence during forming and obtaining useful strain data that can be implemented in forming simulations. This paper explores the applicability of different DIC-based methods, such as Half-Specimen Dome Tests, Sheared Edge Tensile Tests, and KWI hole expansion tests with a flat nosed punch, for characterizing the edge formability of three cold-rolled AHSS sheets. The results obtained from the different testing methods are compared and validated with a laboratory-scale demonstrator. Finally, the limitations and advantages of the different methods are discussed.

1. Introduction

Advanced High Strength Steels (AHSS) have become the dominant material choice for lightweight construction in automotive. Steel is affordable, has good in-service performance, manufacturability, and recyclability. AHSS allow down gauging and, therefore, weight saving, making them the preferred choice over conventional steels. Today, a modern vehicle body contains about 73% of these steels and this percentage will continue to grow in the coming years. In the body structure weight is saved by employing cold rolled galvanised AHSS such as dual phase (DP) and complex phase (CP) steels.

The main drawback is that the high strength achieved in these steel grades is usually associated with limitations in cracking resistance and formability. As a result, during their processing, unexpected defects (cracks, stretching, thinning, etc.), not predicted by traditional experimental or computational approaches at the product design stage, can occur. Because of this, forming parameters and raw material quality must be carefully controlled to assure defect-free part production and guarantee part quality.

Typical metal sheet forming processes for manufacturing AHSS parts includes cutting operations like shearing, blanking or punching. It is well known that these operations produce a shear-affected zone

in the cut edge, with material deformation and damage (work hardening, residual stresses, voids and cracks) [1].

Such damage degrades the edge mechanical properties which locally reduces formability, needed for post-cutting forming operations. In materials with limited ductility such as AHSS, edge damage may trigger edge cracks in sheared areas that expand during forming operations involving stretch flanging or hole expansion. This cracking phenomenon is known in the automotive industry as edge-cracking. Edge-cracking compromises part quality because it cannot be predicted from the part design stage and cracks could appear in part production when cutting parameters or coil properties change.

A significant amount of research work has been done on sheet metal mechanical shearing for conventional steel grades. However, the observed behaviour of AHSS is not always following the same trend as conventional steels where higher ductility means higher edge-crack resistance. It is accepted that edge-cracking resistance in AHSS is related to both the microstructure and the cut edge integrity (presence of cracks) [2, 3]. AHSS with high strength (≥800 MPa) are especially sensitive to the presence of cracks or defects at the sheared edge.

Traditional approaches to characterize formability and mechanical properties in sheet materials do not give sufficient accuracy and reproducibility to properly describe edge fracture and laboratory results cannot be transferred to industrial parts. FLC curves and tensile tests provide only predictions on global formability for restricted conditions like dome stretching but not for local formability modes such as stretch flanging, hole extrusion and tight-radius bending [4]. Local formability failure modes are an entirely different failure condition, where fractures occur from applied concentrated (local) deformation. AHSS grades showing high global formability (DP, TRIP) do not always show high local formability as well.

From the multiple tests available in the literature, the most common and the only standardized one to assess the formability of cut edges on punched sheets is the Hole Expansion Test, ISO16630 [5]. The value obtained in this test is the Hole Expansion Ratio (HER). Large variations in the HER of the same AHSS grades are well known from practical testing experience [6] and have become an obstacle in objectively evaluating the edge-cracking resistance of AHSS. Thus, ISO HET is not suitable for quality control method in a production line and other alternative edge-crack tests as KWI test, hole tension test, or others with the aid of Digital Image Correlation (DIC) systems have been developed. An extensive overview of edge-crack tests found in the literature is given in reference [7]. Nevertheless, and despite all the uncertainties about the applicability of ISO HET to characterize the edge-cracking resistance, the HET closely resembles industrial cases and the method is very easy and fast to perform.

In the present work, the applicability of different DIC-based methods, such as Half-Specimen Dome Tests, Sheared Edge Tensile Tests, and KWI hole expansion tests with flat nosed punch is explored and compared with classical Hole Expansion Tests. All these tests are also compared with a laboratory-scale demonstrator. Finally, the limitations and advantages of these different methods are discussed for the investigated steels.

2. Materials and methods

2.1. Materials

Three cold-rolled AHSS grades with thicknesses between 0.8 and 1.5 mm are analysed in the study: a dual-phase steel (DP1000) and two complex phase steels, CP1000HD and CP1200. Table 1 shows their mechanical properties extracted following ISO6892-1 standard [8] and using specimens type 2 with a reference gage length of 80 mm.

2.2. Experimental methods

2.2.1. Hole Expansion test (HET). These tests were performed according to ISO16630. Squared samples with an initial punched hole of 10 mm diameter in the centre were used (Figure 1a). According to standard recommendations, the hole was punched using a punch-to-die clearance of 12%. The hole expansion was performed using a conical expansion tool with a top angle of 60º (Figure 1b).

Table 1. Mechanical properties of the investigated steels. t, thickness; YS, yield stress; UTS, ultimate tensile strength; UE, uniform elongation; TE, total elongation; n, strain hardening coefficient at uniform elongation (UE); r, anisotropy at 4% elongation.

Steel	t [mm]	Direction	YS [MPa]	UTS [MPa]	UE [%]	TE [%]	n	r_4
DP1000	0.8	Rolling	762	1066	7.7	11.7	0.074	0.84
		45º	736	1048	7.9	11.8	0.076	1.10
		90º	735	1074	7.5	10.5	0.073	0.94
CP1000HD	1.5	Rolling	893	1052	7.3	11.1	0.071	0.91
		45º	905	1052	7.0	10.6	0.068	1.02
		90º	909	1062	7.1	10.7	0.068	0.96
CP1200	1.5	Rolling	1075	1208	5.2	8.3	0.051	0.88
		45º	1076	1206	5.2	7.8	0.051	0.96
		90º	1079	1215	5.1	8.3	0.049	0.92

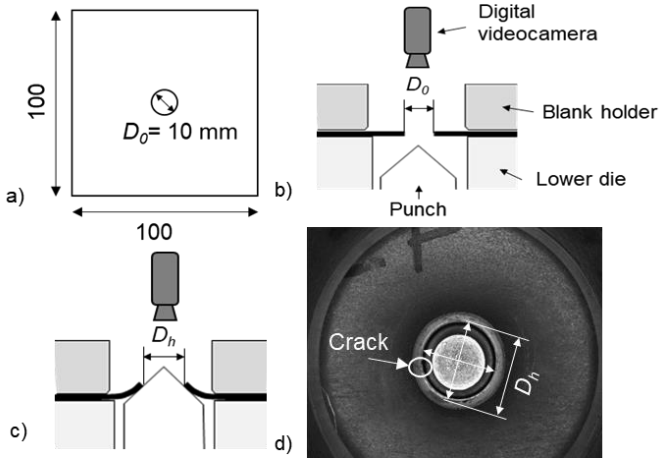

Figure 1. a) Typical specimen geometry used for hole expansion tests. Experimental setup for the determination of the HER before (b) and after (c) the test. d) Image for evaluation of D_h.

The tests were performed simultaneously in three laboratories to show the variability of the test due to coaxiality of the punching tool and the method for crack detection. In Lab1 the tests were conducted in a drawing press at a displacement rate of 0.3-0.5 mm/s without video instrumentation. The tests were stopped manually by naked eye and the measure was done after springback. Tests at Lab2 were performed in a universal testing machine at a displacement rate of 1 mm/s and were stopped after the first trough-thickness crack was observed. Crack occurrence was detected by using a high-resolution video camera (Figure 1b). Finally, a sheet metal testing machine was used by Lab3 at a displacement rate of 0.25 mm/s using a USB camera to judge the appearance of the first crack by the operator. A minimum of 3 specimens per steel were tested. The hole expansion ratio was obtained as follows:

$$\lambda = \frac{D_h - D_0}{D_h} \times 100$$

where λ is the HER, D_h is the hole diameter at crack detection and D_0 is the initial hole diameter. D_h was measured using a calliper by Lab1 and Lab3 in unloaded condition, and from the images of the video camera using a digital image analysis software by Lab 2 in loaded condition (Figure 1d).

2.2.2. KWI Hole Expansion test with flat nosed punch. The ISO HET, though well established and widely used, does by design exhibit a contact force on the edge, which is expected to influence the results, at least for some materials [9]. Sometimes by sheer geometrical influences there is a stretched

flange which has no contact force on the flat surface of the sheet, like in the corner of a bodyside of a car. For that reason, the three materials were also subjected to flat nosed punch test.

The same squared samples of standard HET were used (Figure 2a). The hole expansion was performed using a flat nosed punch (Figure 2b). These tests were performed simultaneously in Lab1 and Lab3. In Lab1, same punch and press equipment as ISO HET were used and tests were also stopped manually by naked eye. The same speed as for conical punch was used (0.5 mm/s). Lab 3 performed all the tests in a universal sheet metal testing machine at a displacement rate of 0.1 mm/s. The tests were stopped after the first trough-thickness crack was observed. In this case, crack initiation was detected by using a high-resolution video camera and strain with DIC.

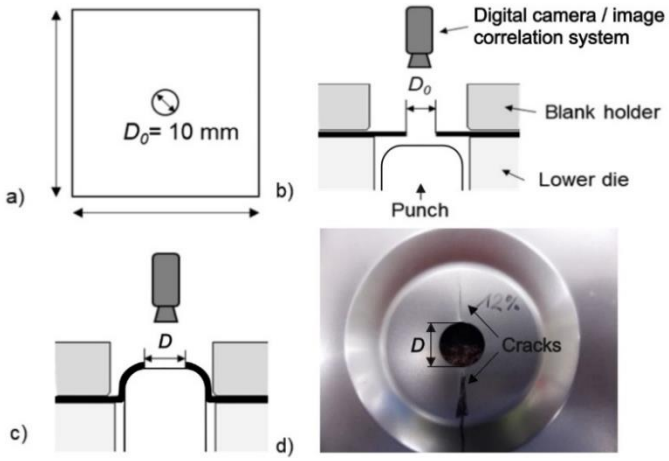

Figure 2. a) Typical specimen geometry used for KWI hole expansion tests. Experimental setup for the determination of the HER before (b) and after (c) the test. d) Image for evaluation of D.

It should be noted that the failure in a flat nosed punch test may originate in the bulk of the material rather than on the edge. This depends on the size of the hole, the clearance, and material properties.

2.2.3. SETi test. Sheared edge tensile improved, where improved is referring to the DIC measurement, was introduced in 2015 [10]. In these uniaxial tensile tests, the sample was a straight strip with both sides sheared, enabling the preparation easier and allowing much more freedom in setting the cutting clearance. The specimen width was 20 mm and the free length was 50 mm. The crosshead displacement rate was 0.5 mm/s and the DIC frequency was 15 Hz.

The tooling was laid out to function on a universal testing machine with good control over force and displacement as well as having good data acquisition. Furthermore, the results could be also compared to ISO and flat nosed punch hole expansion tests. As in previous cases, the cutting clearance used in the test was 12% to compare all the tests carried out. The shearing operation has been carried out at two speeds: 1 mm/s (low); and 100 mm/s (high).

2.2.4. Half Specimen Dome test (HSDT). This test was developed by Shih et al. [11] as an additional approximation to determine the edge cracking behaviour during flanging operations. Shih used it to analyze the edge quality of sheared, waterjet and laser cutting specimens. Compared to hole flanging tests, the half dome test is a more time and cost-saving test for evaluating edge cracking behaviour. HSDT is also unaffected by aspects relating to the manufacture of the tools for punching the holes, as the coaxiality between punch and die. Shih et al. also concluded that shearing angle, tool clearance and anisotropy will also affect edge cracking behaviour.

Figure 3a illustrates the HSDT tools, the same used to determine the FLC. To perform the tests, a DIC system has been used to detect the onset of the first through-thickness crack. The main outputs of HSDT are the dome height (or drawing depth/punch stroke), Figure 3b, and fracture strain of the sheared edge in the previous stage to first crack appears, Figure 3d. To perform HSDT tests, a double-acting hydraulic press was used. The press-holder was equipped with a circular rib to avoid material sliding. All tests were performed at 1 mm/s punch speed.

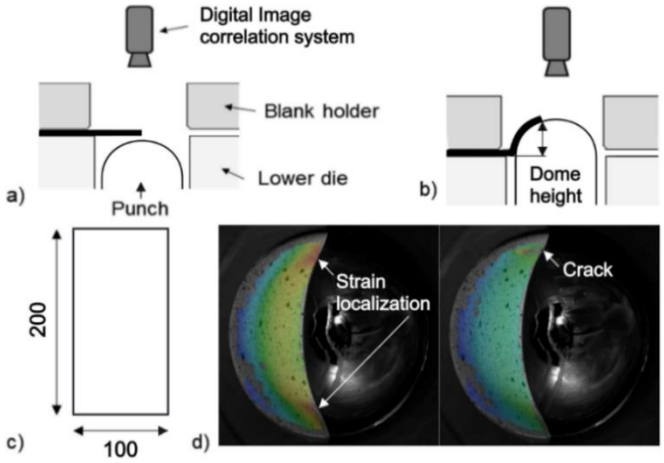

Figure 3. Nakajima tool before (a) and after (b) the test. Specimen geometry used for HSDT (c). DIC image used for evaluation of dome height and strain at previous stage to the appearance of crack (d).

During the tests, it was detected that, although the rib to prevent the specimen from slipping, in some cases this was not effective. In these cases, the dome height obtained is considered to be above the real one, so these values are not always reliable. Thus, in order to have results less dependent on the possible slipping of the specimen, in this article only the values of strain at fracture have been considered.

Regarding specimen identification, the code used for specimen identification is in accordance with the defined in ASTM E399 [12]. Three orientations were performed: L-T (0º), D-D (45º) and T-L (90º). The first letter indicates the orientation of the specimen geometry with respect to the rolling direction, and the second letter indicates the crack propagation direction.

2.2.5. Laboratory-scale demonstrator. The semi-industrial tests have been performed using a S-shape contour tool to test the crack sensitivity of the steels after an open cut. This test was performed in two steps. First, a rectangular blank is cut and after, a curved flange is formed, Figure 4. Depending on the position of the blank, different flange heights and elongations could be achieved. Bending and cutting were performed in the same tool changing the punch and die. Due to the concave contour of the central part of the tool the crack appeared in this area.

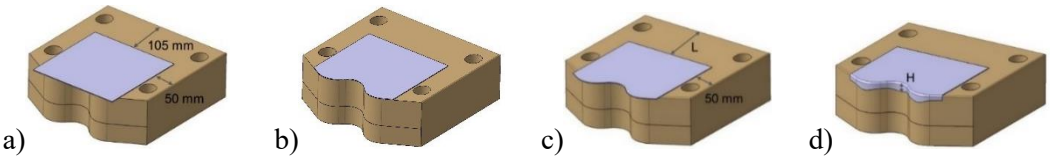

Figure 4. (a) Position of the rectangular blank on the cutting tool, (b) after cutting, (c) positioning the cutting specimen on the bending tool, (d) finished specimen (after flanging).

During cutting the blank is always positioned in the same way on the tool to have the same shaped blank for the further flanging operation. To achieve different flanging heights H, the distance L will be varied in steps of 0.5-1 mm until a crack occurred. To measure the elongation on the edge after forming, the blanks are marked with parallel lines (distance 5 mm) by etching, Figure 5a.

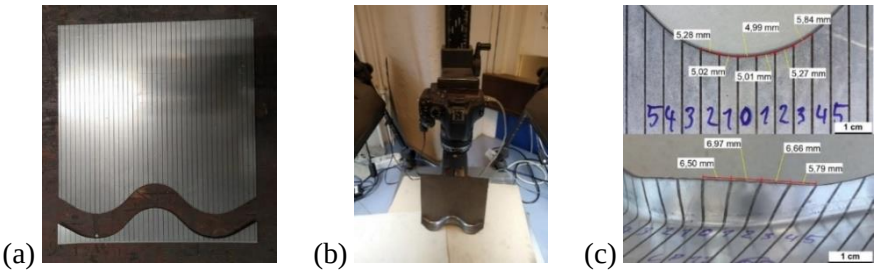

Figure 5. Marked blank with parallel lines (a). Camera setup (b) and optical measurement (c).

After cutting the edge, the length was measured on the blank between these lines. After the test, the deformed edge length was measured again. With these values, the elongation of the edge was calculated. The accuracy of these measurements is limited. The deformed specimen has a 3D contour which will affect the optical measurement. To minimize this failure the specimens were measured in different angles. Figure 5b shows the camera setup and Figure 5c the measurement before and after flanging.

3. Results and discussion

3.1. Hole Expansion tests (HET)

Table 2 shows the hole expansion ratio of the investigated materials in punched 12% clearance for the three laboratories and drilled conditions for Lab1. As clearly seen in this table, drilled HER values are significantly higher than punched ones.

Table 2. Hole Expansion Ratio for the investigated steels.

Steel	Driller conical HER, λ [%]		Punched Conical HER, λ [%]					
			Lab1		Lab2		Lab3	
	Mean	Std. dev.	Mean	Std. dev.	Mean	Std. dev.	Mean	Std. dev.
DP1000	48	7	37	4	27	2	34	3
CP1000HD	126	2	86	5	70	3	-	-
CP1200	137	8	67	5	65	5	59	9

Regarding the values of the punching HER, there are important differences between laboratories. The measurement in Lab2 was carried out with the sample loaded and probably overestimated the elastic contribution in comparison to the fully plastic unloaded condition (Lab1 and Lab3). On the other hand, by measuring the diameter directly on the tool with the video camera, the tests were stopped before in comparison to bare eye operator manual stopping. Thus, both effects should be compensated, and the results can be considered comparable, whereby this is not the main reason for deviations, and scattering probably comes mostly from punching operation.

3.2. KWI Hole Expansion test with flat nosed punch

These tests show that the three steels are not edge crack sensitive at analysed clearance, following in all cases the fractures plane strain paths. In all the tests, the crack starts after some pronounced necking away from cut hole edge, then it propagates to the hole edge. This is however not a classical edge crack. Additionally, the hole diameters have been measured using a calliper, following the ISO way, resulting in mild overshoot in case of large fractures, table 3.

As just said, table 3 illustrates the considerable difference between HER values obtained with ISO and flat nosed punch tests, and that the values are much more similar between the two laboratories than the standard HER tests. In this case, the values obtained with the flat nosed punch test are much lower than those of the standardized HET.

Table 3. Results of flat nosed punch tests with 12% clearance for the investigated steels.

Steel	HER flat nosed punch, λ [%]			
	Lab1		Lab3	
	Mean	Std. dev.	Mean	Std. dev.
DP1000	21	2	22	3
CP1000HD	31	1	-	-
CP1200	21	1	25	1

3.3. SETi test

The SETi tests are evaluated by finding the strain on the edge in the stage just before failure at the position of failure. The failures classified as abrupt are those where failure occurred in one stage of DIC

system measurement, and it cannot be firmly considered as clear edge failure, table 4. Thus, if the strain on the edges for the abruptly failing specimens is trusted, then it seems fast cutting reduces edge ductility. The fuzziness of the results was judged to be mainly due to the uncertainty of where fracture has originated. This is inherent in the simple tensile loading of the test combined with material with relatively good edge ductility, i.e. high HET. The SETi test only worked well for DP1000.

Table 4. Edge failure (major) strain (including abrupt failures).

Steel	Slow cutting				Fast cutting			
	Logarithmic		Technical [%]		Logarithmic		Technical [%]	
	Mean	Std. dev.	Mean	Std. dev.	Mean	Std. dev.	Mean	Std. dev.
DP1000	0.336	0.029	40	3	0.327	0.009	39	1
CP1200	0.567	0.031	76	3	0.428	0.062	53	6

3.4. Half Specimen Dome tests (HSDT)

All HSDT values were extracted from the analysis of the results of the DIC measurements. To obtain the strain coordinates in the sheared edge a curve was made following them to determine the strain as a function of position. The maximum strain values were extracted from this curve, thus locating the two necking zones on the edge of the specimen during the HSDT test, just before the fracture, Figure 3d.

To analyse the strain path followed by the necking zone of HSDT specimens, also a point was situated in the cutting edge. By this point, it was observed that the strain path of the necking zone was uniaxial. Major strain extracted from HSDT is shown in table 5. The burr position was in die side (UP) in the same way as in the HER tests.

Table 5. Edge failure (major) strain in HSDT for the investigated steels.

Steel	Edge direction		Logarithmic		Technical [%]	
	Angle	E399	Mean	Std. dev.	Mean	Std. dev.
DP1000	0º	L-T	0.186	0.038	20	4
	45º	D-D	0.222	0.013	25	1
	90º	T-L	0.151	0.038	16	4
CP1000HD	0º	L-T	0.370	0.016	45	2
	45º	D-D	0.457	0.057	58	6
	90º	T-L	0.417	0.050	52	5
CP1200	0º	L-T	0.400	0.012	49	1
	45º	D-D	0.354	0.037	42	4
	90º	T-L	0.393	0.021	48	2

Table 5 shows the effect of anisotropy in major strain values. In all steels, there is a clear anisotropy effect. Thus, the higher values for DP1000 and CP1000HD are obtained with trimmed edge oriented at 45º from RD. For CP1200 steel, the results of 0º and 90º are quite similar and higher to those of 45º.

3.5. Laboratory-scale demonstrator

The average height and elongation over the rolling direction were calculated to compare the steels. The results of the flange height show a clear ranking. The DP1000 achieve the lowest and the CP1000HD the highest flange height without crack. The same trend is visible in the elongation, Table 6. This table does not show deviation in the results since only one specimen was tested per material and orientation, due to the arduous manual work involved in these measurements.

DP1000 shows the clearest crack occurrence of all materials. The achievable flange height is in diagonal the highest, as already stated by Unruh et al. for this type of steels [13]. Parallel and perpendicular have the same height. Overall, the achievable flange height is the lowest for DP1000.

CP1000HD achieves parallel to the rolling direction the biggest height. Elongation without crack is in diagonal direction slightly higher than parallel. CP1200 shows in the flange height for all three directions comparable values.

Table 6. Flange height and elongation for the investigated steels.

Steel	Edge direction		Results without crack		Results with crack	
	Angle	E399	Height [mm]	Elongation	Height [mm]	Elongation
DP1000	0º	L-T	6.67	0.166	7.53	0.195
	45º	D-D	7.35	0.169	7.70	0.174
	90º	T-L	6.70	0.146	7.40	0.168
CP1000HD	0º	L-T	17.70	0.502	18.80	0.760
	45º	D-D	16.80	0.521	17.95	0.588
	90º	T-L	15.61	0.391	15.95	0.600
CP1200	0º	L-T	13.40	0.391	14.30	0.512
	45º	D-D	12.94	0.321	13.30	0.468
	90º	T-L	13.25	0.320	13.35	0.330

3.6. Test comparison

To compare the different tests aimed at characterizing edge formability, the only one that is standardized, the ISO HET, was initially taken as a reference. To avoid introducing differences in tool design and measurements between the different laboratories, the results of the different tests carried out by the same laboratory are compared, except in the case of semi-industrial tests.

If the ISO HET test is compared with the HET flat nosed punch, the relationship is far from being linear, Figure 6a. This seems logical if one considers that in KWI test the fracture never appeared by the edge. When the comparison is made between the ISO HET and the SETi test, since data is only available for two steels, it is not possible to clearly analyse whether the results show similar trends, or not, Figure 6b. However, it is clear that the cutting speed affects to the maximum edge strain obtained for CP steel. For DP steel this effect is not observed.

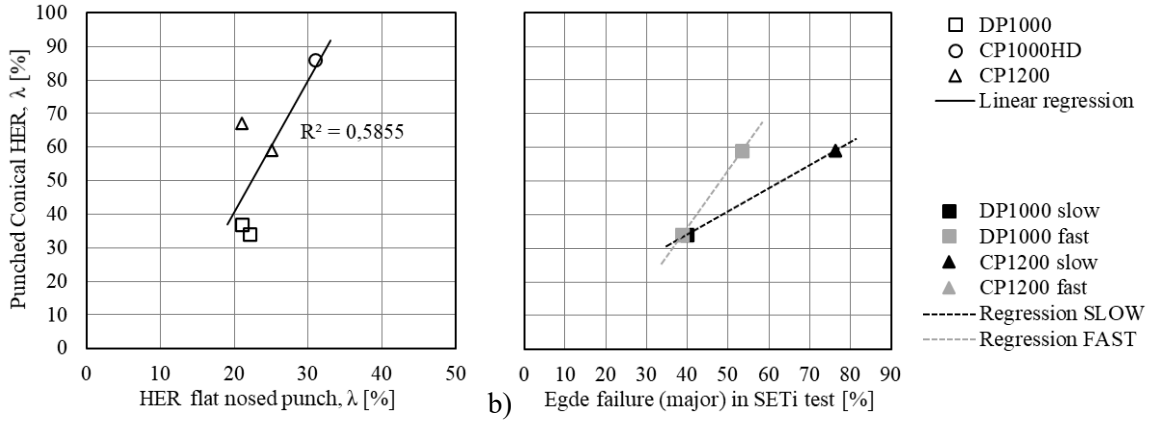

a) b)

Figure 6. ISO HER vs. HER flat nosed punch (a). ISO HER vs. edge failure strain at SETi test (b).

In the case of the relationship between the ISO HET and HSDT tests (Figure 7), the linear relationship is clear, and it is even more evident when only the minimum strain obtained in the HSDT test for each material is represented, Figure 7b. The latter would better represent what actually occurs in the ISO HET, in which the crack appears in the orientation that presents the lowest resistance to edge-cracking.

Since the results between the ISO HET and the HSDT can be considered equivalent, the laboratory-scale demonstrator results are compared only with the HSDT values, Figures 8 and 9. Thus, same edge orientations relative to the rolling direction can be directly compared.

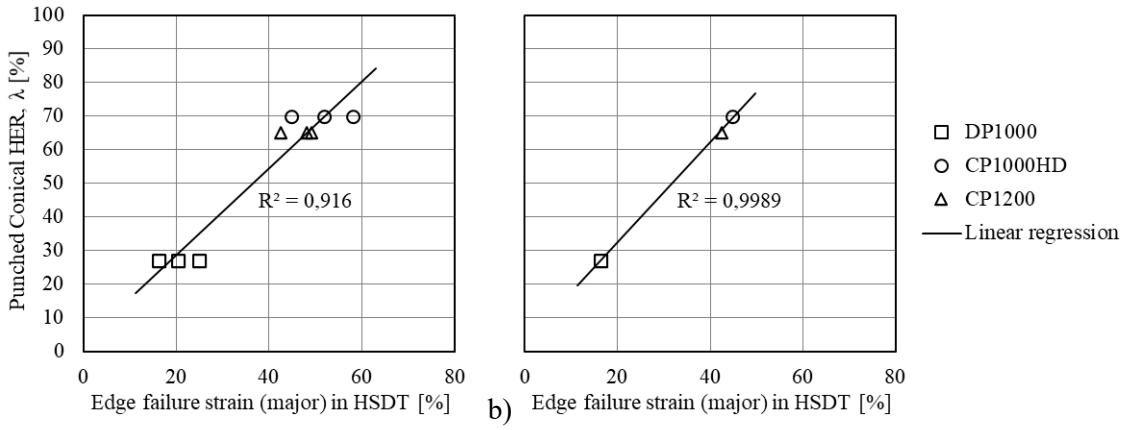

Figure 7. ISO HER vs. edge failure major strain at HSDT test with all data points (all orientations) (a) and only with the lowest value (one orientation) (b).

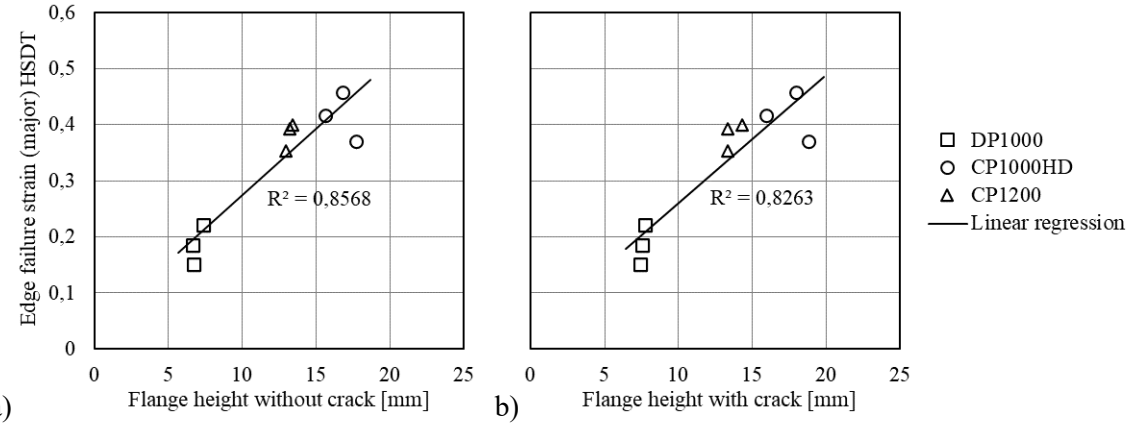

Figure 8. Edge failure major strain at HSDT vs. flange height without crack (a); and with crack (b).

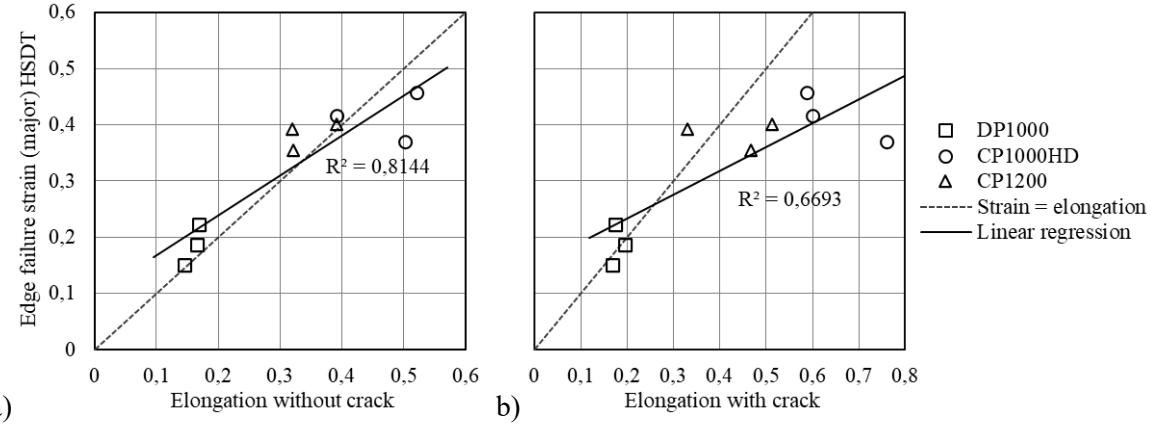

Figure 9. Edge failure major strain at HSDT vs. elongation without crack (a); and with crack (b).

This last comparison, made between the demonstrator specimens with and without cracks, highlights two facts. On the one hand, the relationship between the results of these two tests is clearer when comparing the values of the demonstrator without crack, such as the HSDT results, taken in the previous stage to fracture, Figures 8a and 9a. And on the other, that in this case, the greatest strain obtained in the HSDT is similar to the elongation obtained in the laboratory-scale demonstrator, Figure 9a. It should be considered, however, that the strain measurement and the detection of the previous stage to fracture are sufficiently different between both tests, which would justify the greater dispersion of results in the more industrial test, more evident as the strain increases.

4. Conclusions

After analysing the sheared edge formability of three cold-rolled advanced high strength steels through different tests and a demonstrator, the main conclusions that can be drawn are the following.

- The ISO HET presents notable differences in the results reported by different laboratories for the same steel. These differences, despite the different methods to detect the crack and measure the diameter, can be attributed to punching tool design and wear, nominal tool clearance, cutting punch speed and differences in punch and die coaxiality.
- The flat nosed punch test may be more applicable to certain processes than ISO HET, but failure occurs in the bulk material for the steels and clearance analysed, and then consequently edge condition cannot be assessed. If they compare to each other, seems to be the HER results in flat nosed punch tests are much lower than in ISO HET.
- HET flat test requires therefore more careful sample analysis in comparison to ISO conical test where crack almost always start at hole edge. By post-mortem sample inspection with or without necking it can be roughly estimated if the crack starts from the edge or from bulk material.
- SETi test is unsuitable to obtain clear local fracture strains in case the materials exhibit relative good local ductility. Due to this it could not be established if the trend in local fracture strains coincides with that in global fracture strains such as provided by ISO HET and flat nosed punch tests. To determine the influence of cutting speed further testing is required.
- HSDT test allows detecting the effect of material anisotropy in edge-cracking, which cannot be measured by HET. The ISO HET and HSDT show a linear relationship. Linearity that is more evident when only the minimum strain obtained in the HSDT for each material is represented.
- The results of the HSDT and laboratory-scale demonstrator tests show a clear relationship, especially when comparing of the demonstrator samples before the appearance of cracks. The lower-than-expected linearity may be caused by the difficulties with the measurement of the elongation on the edge due to the 3D contour of the flanged specimen. In this case, in which the strain measurement is manual and not automatic as in the HSDT, the accuracy depends on the experience of the operator.

It is necessary to comment, however, that these results are obtained from only 3 cold-rolled steels, for which it is necessary to extend them to more steels to confirm the observed trends.

Acknowledgments

The authors gratefully acknowledge the funding received by the Research Fund for Coal and Steel programme (847213-CuttingEdge4.0-RFCS-2018).

References

[1] Levy B S and Van Tyne C J 2012 *J. Mater. Eng. Perform.* **21** pp 1205-13
[2] Gutiérrez D, Escaler J, Lara A, Casellas D and Prado J M 2011 *Proc. IDDRG2011 Conf.* (Bilbao)
[3] Lara A, Frómeta D, Molas S, Rehrl J, Suppan C and Casellas D 2016 *Proc. IDDRG2016 Conf.* (Linz) pp 499-509
[4] World Auto Steel 2021 *AHSS Application Guidelines* version 7.0
[5] ISO16630 2017 Metallic materials – Method of hole expanding test
[6] Larour P, Pauli H, Freudenthaler J, Lackner J, Leomann F and Schestak G 2016 *Proc. IDDRG2016 Conf.* (Linz) pp 480-98
[7] Schneider M, Geffert A, Peshekhodov I, Bouguecha A and Behrens B A 2015 *Mater. Sci. Technol.* **46** pp 1196-217
[8] ISO6892-1 2019 Metallic materials - Tensile testing - Part 1: Method of test at room temperature
[9] Ooms B R J 2017 *MSc thesis, University of Twente*
[10] Atzema E and Seda P 2015 *Forming Technology Forum 2015* (Zurich)
[11] Shih H C, Hsiung C K and Wendt B 2014 *SAE Technical Paper* **2014- 01-0994**
[12] ASTM E399 Standard Test Method for Plane-Strain Fracture Toughness of Metallic Materials
[13] Unruh K and Heuse M 2017 *Steels in Cars and Trucks Conf.* (Amsterdam)